

## Age and Petrochemistry of Bahrah Granodiorite-Granite Complex, Jeddah-Makkah Region, Saudi Arabia

A.A. RADAIN, A.M.S. AL-SHANTI and A.A. ABDEL-MONEM\*  
*Faculty of Earth Sciences, King Abdulaziz University,  
Jeddah, Saudi Arabia.*

**ABSTRACT.** The Bahrah granodiorite-granite complex is an oval intrusion oriented NE-SW forming a negative geomorphologic feature at the intersection of Wadi Fatima to the west and Wadi Al-Shumaysi to the east. It is bound to the west by Jeddah group metavolcanics and Bahrah group paraschist. To the east, it is in contact with Jeddah group metavolcanics and intruded quartz-diorites. The complex is traversed by fine grained basic dikes trending E-W.

The rock types range from gabbroic to granitic. The main rock type is medium to coarse grained biotite and sometimes biotite-hornblende granite. The quartz-diorite and granodiorite facies near the eastern borders of the complex are slightly foliated and contain abundant mafic xenoliths, indicating an emplacement mechanism by stoping.

The intrusion is peraluminous calc-alkaline in nature and highly depleted in LIL-elements suggesting a subduction related origin of the magma. The Rb/Sr age obtained is  $665 \pm 12$  Ma, and is interpreted as the age of emplacement during post-Fatima group time whose age is 690-680 Ma. This is the time-equivalent of the post-Halaban-Hulayfah tectono-plutonic cycle widely spread in the Arabian Shield.

### Introduction

The Jeddah-Makkah region is located in western Saudi Arabia between latitudes  $21^{\circ}00'$ - $21^{\circ}30'N$  and longitudes  $39^{\circ}00'$ - $39^{\circ}45'E$ . It was one of the earliest areas to be studied geologically in the Arabian Shield (Brown *et al.* 1963). The area triggered further investigations since Aldrich (1978) reported ages ranging between 720-1025 Ma for some gneissic units in the area. Later, Skiba (1980) compiled the regional geologic mapping of the area and designated the oldest lithostratigraphic unit as the

---

*Present Address:* Nuclear Materials Authority, P.O. Box 530, Maadi, Cairo, Egypt.

Arafat group, which comprises a sequence of sedimentary pyroclastic and volcanic rocks that are tightly folded and intensely metamorphosed in the amphibolite facies. The early plutonic intrusions are represented by foliated rocks which are inter-layered with members of the Arafat group and arc of variable composition. They range from gabbros, diorites, quartz-diorites, tonalites, biotite-granodiorite, to biotite-granites.

The second or later phase of plutonic intrusions includes all plutonic bodies that cut the Arafat and later stratigraphic units in the area. The early phases of intrusions comprise large amounts of diorite, quartz-diorites and tonalites. Plutonism continued with the emplacement syntectonically of tonalites to granodiorites of plutonic to batholithic sizes. This orogenic (Hijaz)-cycle ended with a late-tectonic and post-tectonic intrusions which range in composition from granodiorite to granite.

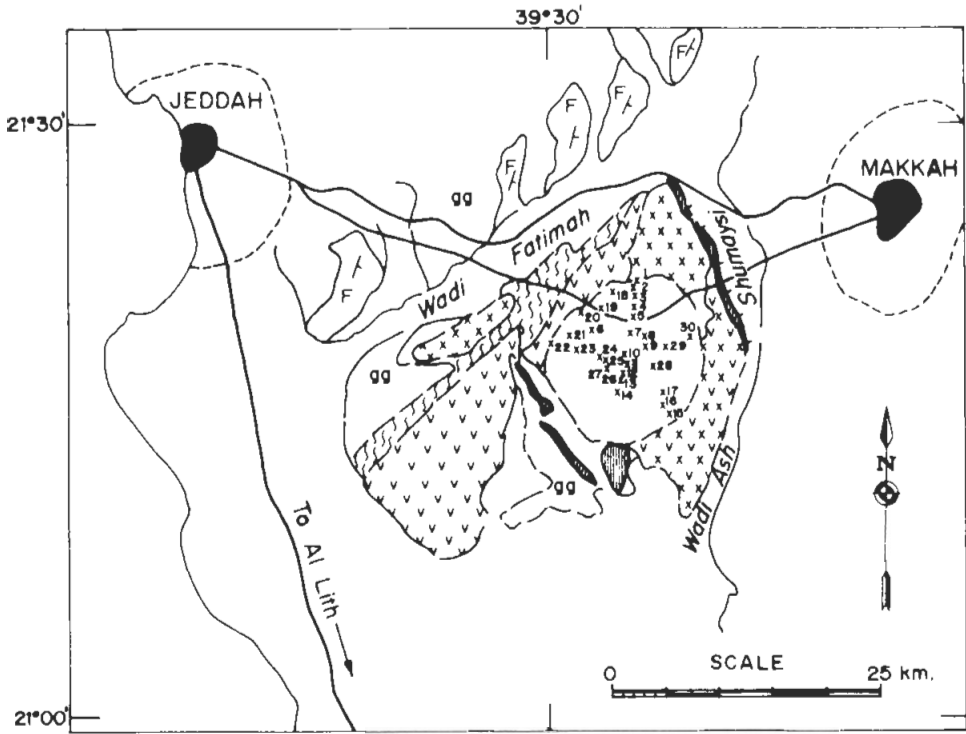
Fleck *et al.* (1980) reported Rb/Sr ages from the Jeddah area that contradicted the ages reported earlier by Aldrich (1978). Further, Fleck (1981) reported Rb/Sr ages of dioritic to granitic plutons in the Jeddah-Makkah region ranging between 700 and 820 Ma, with a cluster between 760-780 Ma. Also, he observed a very low initial  $^{87}\text{Sr}/^{86}\text{Sr}$  ratios ( $\sim 0.702$ - $0.703$ ) in all the plutons dated. These low initial ratios and the calc-alkaline chemical nature of the plutonic rocks of the area reported by Skiba (1980), led to the suggestion that the area was developed within ensimatic environment at a convergent plate-margin.

In this paper, we are investigating, in detail, the petrochemistry of the Bahrah granodiorite-granite complex (Jeddah-Makkah area) as well as presenting its Rb/Sr-isochron age. This pluton, which shows circular outlines with little evidence of deformation and exhibiting negative topographic features, represents the syn- to late-tectonic type of intrusions. It is intended to examine the tectonic setting within which this plutonic complex evolved as well as the time-span of plutonic activity in the area. Also, it is intended to correlate the age and chemistry of this plutonic intrusion with similar ones from other areas in the Arabian Shield.

### Geologic Setting

The Bahrah granodiorite-granite complex is a semi-circular pluton about 10 km in diameter (Fig. 1). It forms low relief lands at the intersection of Wadi Fatima to the west and Wadi Al-Shumaysi to the east. It is bound to the west by a narrow ridge of Jeddah group metavolcanics which is separated from the Fatima metavolcanic-metasedimentary series by a zone of paraschist of the Bahrah group, (Fig. 1). To the east, the pluton is in contact with Jeddah group metavolcanics and intrusive quartz-diorite. Chilled margin facies against the western metavolcanics have been observed. From the north, the pluton is bound by the foliated biotite granodiorite complex of Makkah batholith.

In the field, the rock types range from gabbroic to granitic. The main rock types are medium to coarse grained biotite-hornblende-granodiorite and biotite-granite. Limited exposures of dark black gabbros and diorites in the form of small hills standing astride the low relief granitic terrains are present. Biotite-hornblende granodior-



**LEGEND**

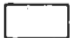

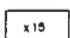
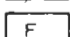
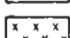
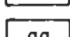
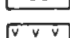
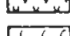
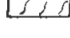
-  Alluvium
-  Shumaysi formation
-  Bahrah pluton
-  Fatimah series
-  Granodiorite (Makkah batholith)
-  Granite gneiss
-  Metavolcanics (Jeddah group)
-  Chlorite sericite schist (Bahah group)
-  Sample location and number

FIG. 1. Geologic map of Bahrah area.

ite with mafic xenoliths is present near the center of the pluton. Fine grained basic dikes trending E-W cut the granite. The quartz-diorite and granodiorite facies near the eastern borders of the pluton are slightly foliated and contain abundant mafic xenoliths. Near the center of the pluton pink microgranites occur in the form of small plugs, veins and dikes. The biotite-granite is epidotized in places. Also, the hornblende is sometimes altered to actinolite, whereas the biotite is sometimes altered to chlorite.

### Petrography and Petrochemistry

The Bahrah granodiorite-granitic complex was sampled along two main traverses, one along the N-S direction and the second across the E-W direction (Fig. 1). In all, 42 samples were collected as fresh as possible and representing almost all the rock varieties of the complex. The rocks have been studied petrographically in thin sections and chemically analysed for major elements as well as some trace elements, Rb, Sr, Ba, Y, Nb, and Zr. The analytical results are shown in Table 1.

TABLE 1. Chemical analyses and CIPW norms of Bahrah granodiorite-granite complex.

Sample No.	MK-1	MK-2	MK-3	MK-4	MK-5	MK-6	MK-7	MK-8	MK-9
SiO <sub>2</sub>	67.53	67.81	67.10	67.20	67.62	67.73	74.86	69.91	66.78
TiO <sub>2</sub>	0.40	0.36	0.36	0.40	0.32	0.38	0.27	0.26	0.43
Al <sub>2</sub> O <sub>3</sub>	13.55	14.03	14.86	13.80	15.05	14.87	12.25	14.66	13.54
Fe <sub>2</sub> O <sub>3</sub>	2.10	1.97	2.04	2.33	1.65	1.40	1.06	1.47	2.17
FeO	2.24	1.80	1.91	1.75	1.59	1.54	0.77	1.12	2.79
MnO	0.10	0.08	0.09	0.08	0.08	0.05	0.02	0.06	0.12
MgO	1.80	1.23	1.19	1.44	1.33	1.22	0.24	0.82	2.04
CaO	4.25	4.24	4.21	3.86	3.96	3.59	1.62	3.48	4.86
Na <sub>2</sub> O	3.01	3.21	3.44	3.97	4.05	4.30	4.36	3.82	3.13
K <sub>2</sub> O	1.61	2.11	2.00	2.09	2.10	1.98	2.42	1.88	1.96
P <sub>2</sub> O <sub>5</sub>	0.09	0.09	0.09	0.09	0.09	0.08	0.07	0.08	0.09
H <sub>2</sub> O <sup>+</sup>	1.70	0.92	0.84	0.86	0.68	0.79	0.51	0.72	0.70
H <sub>2</sub> O	0.13	0.18	0.17	0.12	0.14	0.13	0.16	0.12	-
Total	98.51	98.03	99.30	97.99	98.66	98.06	98.61	98.40	98.61
Trace elements in parts/10 <sup>6</sup>									
Nb	10	10	10	11	10	11	12	11	7
Zr	122	117	117	126	126	168	159	126	108
Y	18	18	19	19	18	19	19	19	18
Sr	252	241	265	251	253	373	130	224	237
Rb	51	69	77	75	65	59	58	58	79
Ba	448	448	449	525	488	412	1153	338	450
CIPW									
q	31.84	30.44	28.50	26.65	25.79	25.74	36.73	31.80	27.96
or	9.51	12.47	11.82	12.35	12.41	11.70	14.30	11.11	11.58
ab	25.47	27.16	29.11	33.59	34.27	36.39	36.89	32.32	26.49
an	18.71	17.64	19.20	13.66	16.69	15.43	6.71	16.74	17.11
c	0.00	0.00	0.00	0.00	0.00	0.00	0.00	0.21	0.00

TABLE I. (Contd)

Sample No.	MK-10	MK-11	MK-12	MK-13	MK-14	MK-15	MK-16	MK-17	MK-17A
di	1.44	2.26	0.89	3.89	1.90	1.50	0.69	0.00	5.21
hy	5.69	3.21	3.93	2.52	3.58	3.46	0.40	2.57	5.39
mt	3.04	2.86	2.96	3.38	2.39	2.03	1.54	2.13	3.15
il	0.76	0.68	0.68	0.76	0.61	0.72	0.51	0.49	0.82
ap	0.21	0.21	0.21	0.21	0.21	0.19	0.16	0.19	0.21
Rb/Sr	0.202	0.286	0.291	0.299	0.257	0.158	0.446	0.259	0.333
K/Rb	262	254	216	231	268	279	346	269	206
A/CNK	0.94	0.92	0.96	0.87	0.93	0.94	0.96	1.0	0.84
SiO <sub>2</sub>	69.90	62.08	72.87	69.57	71.12	72.45	73.75	73.96	70.12
TiO <sub>2</sub>	0.35	0.74	0.19	0.47	0.37	0.26	0.22	0.20	0.21
Al <sub>2</sub> O <sub>3</sub>	13.45	17.07	13.60	14.72	13.21	12.54	12.21	13.67	12.48
Fe <sub>2</sub> O <sub>3</sub>	1.59	2.38	0.88	1.50	1.10	1.26	0.92	0.63	0.27
FeO	2.19	2.92	0.61	1.80	1.78	0.97	1.31	1.15	1.09
MnO	0.08	0.09	0.03	0.02	0.06	0.04	0.07	0.06	0.06
MgO	1.32	2.01	0.17	0.95	1.01	0.96	0.61	0.50	0.50
CaO	3.91	5.64	1.62	4.54	3.35	1.62	2.15	2.31	2.40
Na <sub>2</sub> O	3.60	4.43	3.75	3.97	3.82	3.82	4.28	3.82	6.88
K <sub>2</sub> O	2.05	1.48	3.10	1.22	2.38	3.40	2.97	2.83	2.54
P <sub>2</sub> O <sub>5</sub>	0.09	0.11	0.07	0.09	0.08	0.06	0.07	0.07	0.07
H <sub>2</sub> O <sup>+</sup>	0.83	0.92	0.84	0.77	0.57	0.43	0.82	0.75	0.92
H <sub>2</sub> O	-	0.06	0.02	0.05	0.02	0.04	0.06	0.20	0.13
Total	98.36	99.93	97.75	99.67	98.87	97.85	99.44	100.15	97.67
Trace elements in parts/10 <sup>6</sup>									
Nb	11	10	12	9	9	10	10	11	10
Zr	117	145	122	182	150	131	131	154	163
Y	19	19	21	15	16	30	21	17	18
Sr	202	518	131	387	285	108	246	327	300
Rb	66	56	75	47	69	84	91	93	81
Ba	588	450	488	438	488	638	563	826	750
CIPW									
q	30.92	15.88	35.60	31.00	31.40	32.44	32.58	34.79	20.73
or	12.12	8.75	18.32	7.21	14.07	20.09	17.55	16.72	15.01
ab	30.46	37.49	31.73	33.59	32.32	32.32	36.22	32.32	50.05
an	14.49	22.32	7.58	18.74	11.87	7.03	5.33	11.00	0.00
c	0.00	0.00	1.30	0.00	0.00	0.00	0.00	0.29	0.00
di	3.53	3.99	0.00	2.59	3.46	0.49	4.02	0.00	6.01
hy	3.84	5.42	0.56	2.43	2.68	2.55	0.94	2.62	0.00
wo	0.00	0.00	0.00	0.00	0.00	0.00	0.00	0.00	1.78
ac	0.00	0.00	0.00	0.00	0.00	0.00	0.00	0.00	0.78
mt	2.31	3.45	1.28	2.17	1.59	1.83	1.33	0.91	0.00
il	0.66	1.41	0.36	0.89	0.70	0.49	0.42	0.38	0.40
ap	0.21	0.25	0.16	2.21	0.19	0.14	0.16	0.16	0.16
Rb/Sr	0.327	0.108	0.573	0.121	0.242	0.778	0.370	0.284	0.270
K/Rb	258	219	243	215	286	336	271	253	260
A/CNK	0.88	0.89	1.09	0.91	0.88	0.97	0.86	1.01	0.68

TABLE 1. (Contd)

Sample No.	MK-18	MK-19	MK-20	MK-21	MK-22	MK-23	MK-24	MK-25	MK-26
SiO <sub>2</sub>	47.88	68.85	69.68	74.80	75.53	68.40	46.26	74.66	73.92
TiO <sub>2</sub>	0.42	0.33	0.32	0.21	0.17	0.42	1.00	0.24	0.08
Al <sub>2</sub> O <sub>3</sub>	12.87	13.62	13.62	11.80	12.18	12.43	22.43	14.83	13.51
Fe <sub>2</sub> O <sub>3</sub>	3.14	1.71	1.80	0.58	0.80	2.35	2.99	1.61	0.61
FeO	5.22	1.50	1.37	0.08	0.27	2.08	5.15	0.27	0.05
MnO	0.18	0.09	0.08	0.04	0.02	0.10	0.10	0.01	0.01
MgO	8.34	1.15	0.97	1.44	0.29	1.80	2.99	0.18	0.07
CaO	10.07	3.63	3.95	1.68	1.78	4.94	12.62	0.38	0.38
Na <sub>2</sub> O	1.68	3.82	3.78	5.65	3.97	4.36	2.60	1.07	3.68
K <sub>2</sub> O	1.62	1.82	1.92	1.18	2.22	0.96	0.31	2.85	5.07
P <sub>2</sub> O <sub>5</sub>	0.15	0.08	0.08	0.06	0.06	0.10	0.17	0.05	0.05
H <sub>2</sub> O <sup>+</sup>	5.82	1.63	1.77	1.92	2.33	1.84	1.58	1.86	0.69
H <sub>2</sub> O	1.11	0.17	0.16	0.18	0.10	0.10	0.12	0.11	0.19
Total	98.50	98.40	99.50	99.62	99.72	99.88	98.32	98.12	98.31
Trace elements in parts/10 <sup>6</sup>									
Nb	7	10	10	12	8	9	7	11	11
Zr	109	122	122	131	113	136	117	156	95
Y	16	19	175	25	19	13	13	18	25
Sr	596	200	241	110	87	334	876	27	39
Rb	87	53	61	35	62	25	34	70	88
Ba	263	376	450	300	376	263	150	750	338
CIPW									
q	0.96	30.57	31.35	32.83	39.86	28.42	0.00	56.59	32.33
or	9.57	10.76	11.35	6.97	13.12	5.67	1.83	16.84	29.96
ab	14.22	32.32	31.99	47.81	33.59	36.89	22.00	09.05	31.14
an	22.79	14.64	14.53	3.35	8.44	11.51	48.62	1.56	1.56
c	0.00	0.00	0.00	0.00	0.15	0.00	0.00	9.41	1.40
di	20.96	2.28	3.63	3.37	0.00	9.87	10.55	0.00	0.00
hy	17.37	2.74	1.34	2.02	0.72	1.13	4.80	0.45	0.17
ol	0.00	0.00	0.00	0.00	0.00	0.00	2.19	0.00	0.00
mt	4.55	2.48	2.61	0.00	0.44	3.41	4.34	0.21	0.00
il	0.80	0.63	0.61	0.25	0.32	0.80	1.90	0.46	0.12
ap	0.35	0.19	0.19	0.14	0.14	0.23	0.39	0.12	0.12
Rb/Sr	0.146	0.265	0.253	0.318	0.713	0.075	0.038	2.593	2.256
K/Rb	155	285	261	280	297	319	77	338	478
A/CNK	0.56	0.92	0.88	0.87	1.0	0.72	0.81	2.68	1.11
SiO <sub>2</sub>	73.92	48.62	76.65	61.39	52.27	63.00	71.30	67.37	47.08
TiO <sub>2</sub>	0.09	0.44	0.17	1.10	1.65	0.43	0.24	0.22	1.52
Al <sub>2</sub> O <sub>3</sub>	13.54	10.83	12.60	16.45	16.02	15.77	14.10	16.67	19.08
Fe <sub>2</sub> O <sub>3</sub>	1.15	1.68	1.30	1.95	1.92	2.45	1.46	1.84	4.05
FeO	0.23	8.31	0.33	4.26	7.62	2.24	0.63	0.71	6.56
MnO	0.05	0.25	0.02	0.14	0.19	0.11	0.05	0.06	0.14
MgO	0.17	11.76	0.09	1.97	4.06	1.78	0.52	0.44	2.99
CaO	1.81	12.67	0.78	6.66	9.35	5.17	2.37	3.35	12.25
Na <sub>2</sub> O	3.05	2.21	4.66	5.05	4.28	3.97	4.28	3.97	3.05

TABLE I. (Contd)

Sample No.	MK-27	MK-28	MK-29	MK-30	MK-30A	MK-31	MK-32	MK-33	MK-34
K <sub>2</sub> O	3.02	0.54	3.67	0.39	0.26	1.47	2.17	2.90	0.32
P <sub>2</sub> O <sub>5</sub>	0.06	0.18	0.05	0.12	0.15	0.10	0.07	0.08	0.17
H <sub>2</sub> O <sup>+</sup>	0.75	0.97	0.48	0.41	0.63	1.64	0.84	1.46	1.16
H <sub>2</sub> O	0.12	0.14	0.18	0.12	0.18	0.13	0.11	0.12	0.15
Total	97.96	98.6	100.97	100.01	98.58	98.26	98.14	99.19	98.52
Trace elements in parts/10 <sup>6</sup>									
Nb	11	6	11	9	7	4	12	10	6
Zr	130	61	130	251	130	117	117	199	113
Y	37	12	21	16	16	18	40	19	12
Sr	54	370	47	750	723	266	150	606	931
Rb	78	43	51	23	32	52	50	100	33
Ba	901	75	750	215	263	412	338	482	150
CIPW									
q	40.66	0.00	34.03	13.95	0.82	21.00	32.44	25.57	0.00
or	17.85	3.19	21.69	2.30	1.54	8.69	12.82	17.14	1.89
ab	25.81	18.49	39.43	42.73	36.22	33.59	36.22	33.59	25.81
an	8.59	18.04	2.63	21.07	23.73	20.87	11.30	16.10	37.43
ne	0.00	0.11	0.00	0.00	0.00	0.00	0.00	0.00	0.00
c	2.11	0.00	0.00	0.00	0.00	0.00	0.57	1.10	0.00
di	0.00	35.27	0.48	9.24	17.93	3.31	0.00	0.00	18.31
hy	0.42	0.00	0.00	4.99	11.27	4.43	1.29	1.10	3.93
wo	0.00	0.00	0.12	0.00	0.00	0.00	0.00	0.00	0.00
ol	0.00	18.70	0.00	0.00	0.00	0.00	0.00	0.00	0.69
mt	0.64	2.44	0.62	2.83	2.78	3.55	1.50	1.85	5.87
il	0.17	0.84	0.32	2.09	3.13	0.82	0.46	0.42	2.89
ap	0.14	0.42	0.12	0.28	0.35	0.23	0.16	0.19	0.39
Rb/Sr	1.444	0.166	1.085	0.031	0.044	0.195	0.333	0.165	0.035
K/Rb	321	104	597	141	67	235	360	241	80
A/CNK	1.17	0.40	0.97	0.79	0.66	0.90	1.03	1.06	0.69
SiO <sub>2</sub>	68.99	48.53	47.63	65.73	64.06	66.93	47.08	67.88	
TiO <sub>2</sub>	0.28	0.87	0.43	0.40	0.62	0.47	1.33	0.27	
Al <sub>2</sub> O <sub>3</sub>	16.05	22.50	19.95	15.89	15.07	14.80	16.90	13.45	
Fe <sub>2</sub> O <sub>3</sub>	1.47	3.91	1.63	1.65	2.58	1.92	4.30	2.07	
FeO	1.30	3.58	4.38	1.87	2.66	2.12	6.70	1.58	
MnO	0.07	0.08	0.12	0.07	0.08	0.07	0.18	0.09	
MgO	0.48	2.81	7.48	1.23	2.25	1.32	7.06	1.63	
CaO	3.98	13.16	13.84	3.68	4.91	3.87	9.71	4.08	
Na <sub>2</sub> O	3.97	2.52	2.21	4.77	4.27	4.49	3.77	3.52	
K <sub>2</sub> O	1.04	0.40	0.26	2.24	1.94	2.32	0.36	1.40	
P <sub>2</sub> O <sub>5</sub>	0.08	0.18	0.19	0.08	0.10	0.09	0.15	0.09	
H <sub>2</sub> O <sup>+</sup>	0.73	1.06	0.92	0.88	1.11	1.59	1.60	1.93	
H <sub>2</sub> O <sup>-</sup>	0.14	0.08	0.10	0.10	0.16	0.08	0.26	0.14	
Total	99.58	98.68	99.14	98.54	99.81	100.02	99.40	98.13	

TABLE I. (Contd)

Sample No.	MK-35	MK-36	MK-37	MK-38	MK-39	MK-40	MK-41	MK-42
Trace elements in parts/10 <sup>6</sup>								
Nb	11	8	7	10	9	10	7	10
Zr	130	130	105	151	138	143	82	130
Y	18	11	14	18	16	17	14	15
Sr	248	904	591	355	459	336	448	356
Rb	38	33	23	67	73	77	32	48
Ba	263	150	113	675	563	525	150	375
CIPW								
q	32.52	2.81	0.00	19.73	18.96	22.30	0.00	31.34
or	6.15	2.36	1.54	13.24	11.46	13.71	2.13	8.27
ab	33.59	21.32	18.70	40.36	36.13	37.99	28.88	29.79
an	19.22	48.90	43.75	15.33	16.23	13.38	28.13	16.77
ne	0.00	0.00	0.00	0.00	0.00	0.00	1.64	0.00
c	1.35	0.00	0.00	0.00	0.00	0.00	0.00	0.00
di	0.00	12.15	18.97	1.95	6.00	4.24	15.34	2.30
hy	2.04	3.25	0.80	3.66	4.61	2.89	0.00	3.88
ol	0.00	0.00	10.75	0.00	0.00	0.00	12.32	0.00
mt	2.13	5.67	2.36	2.39	3.74	2.78	6.23	3.00
il	0.53	1.65	0.82	0.76	1.18	0.89	2.53	0.51
ap	0.19	0.42	0.44	0.19	0.23	0.21	0.35	0.21
Rb/Sr	0.153	0.037	0.039	0.189	0.159	0.229	0.071	0.135
K/Rb	227	101	94	277	221	250	93	242
A/CNK	1.08	0.79	0.69	0.93	0.84	0.88	0.70	0.91

Petrographically, the complex comprises mainly quartz-diorite facies near its eastern borders, granodiorite covering most of the central and southwestern parts, and granites mostly towards the northern and southern parts. The quartz-diorite is coarse grained, holocrystalline showing well developed intergrowths of quartz and locally present turbid alkali feldspar along with plagioclase, biotite, hornblende and Fe-Ti oxides. The granodiorites consist of about 50% of slightly sericitized K-feldspar and plagioclases, the rest is composed of quartz, and more than 10% biotite, Fe-Ti oxides and green amphibole. The granitic phase consists mainly of hypidiomorphic rocks with perthitic feldspar, lesser plagioclase, and brown biotite slightly chloritized along with intergrowths of quartz and alkali feldspar.

### Major Elements

The normative mineral contents of all the samples from the Bahrah complex are partially shown on Ab-Or-An ternary diagram (Fig. 2). The fields are after Barker (1979). Most of the data plot in the tonalite and granodiorite fields. Few data points plotted in the granite field are indicating the dominance of the granodioritic component in the complex. The Q-Ab-Or ternary diagram (Fig. 3) indicates that the data plotted fall in a field close to the trajectories of 1-5 Kb water pressure. The field of



group III younger granitoids of the Arabian Shield (Jackson *et al.* 1984a,b) is shown for comparison. These syn- to late-tectonic intrusions are of the same age as the group III younger granitoids as will be shown later.

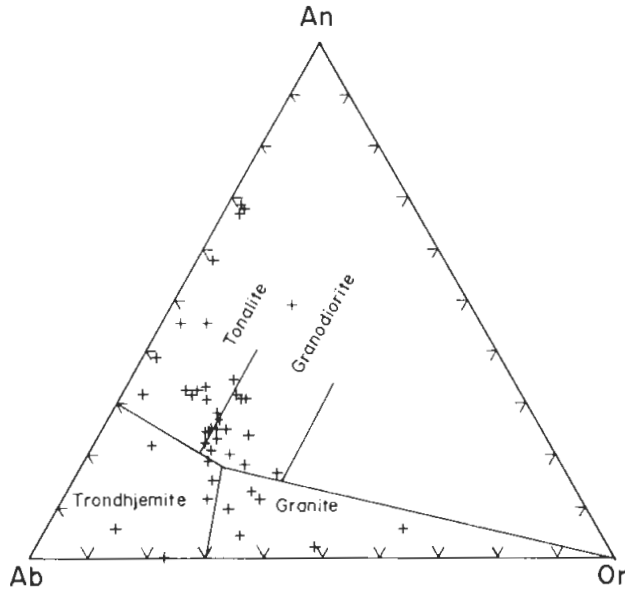


FIG. 2. Normative plot of An-Ab-Or. The field boundaries are from Barker (1979).

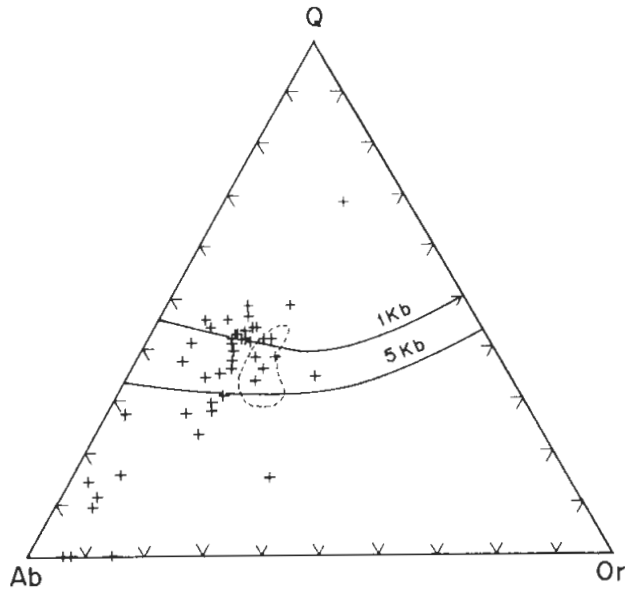


FIG. 3. Normative Q-Ab-Or diagram. The cotectic surfaces for 1 and 5 Kb  $\text{PH}_2\text{O}$  are from Tuttle and Bowen (1958).

The AFM diagram (Fig. 4), shows that all the data investigated fall in the calc-alkaline field using the boundary line suggested by Irvine and Baragar (1971). Some of the dioritic and quartz dioritic samples show some Fe-enrichment. The dashed line on the diagram indicates the position of the calc-alkaline trend designated by Skiba (1980) for the plutonic rocks of the Jeddah-Rabigh area, which is consistent with our data, confirming the calc-alkaline nature of the Bahrah complex. Also, the field of type III younger granitoids of the Arabian Shield (Jackson *et al.* 1984a,b) is shown for comparison.

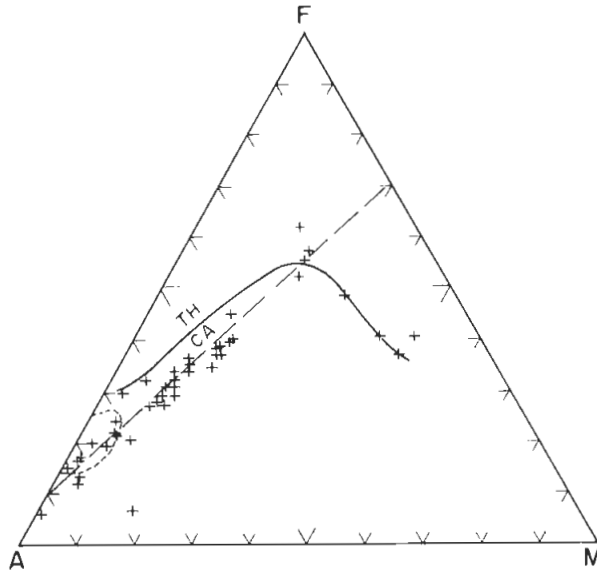


FIG. 4. Data plotted on AFM diagram (A =  $\text{Na}_2\text{O} + \text{K}_2\text{O}$ ; F = total iron as FeO; M = MgO). The line marked by TH/CA shows the boundary between tholeiitic and calc-alkaline rocks, after Irvine and Baragar (1971). Big dashed line shows the plutonic trend of Jeddah-Rabigh area (Skiba, 1980). Small dashed line encloses group III granite (Jackson *et al.* 1984a).

The molar  $\text{Al}_2\text{O}_3/(\text{CaO} + \text{Na}_2\text{O} + \text{K}_2\text{O}(\text{A}/\text{CNK}))$  versus  $\text{Al}_2\text{O}_3/(\text{Na}_2\text{O} + \text{K}_2\text{O}(\text{A}/\text{NK}))$  diagram (Fig. 5), derived from Shand's index (Shand 1951), exhibits the domination of metaluminous nature of the Bahrah Complex rocks. Some samples show peraluminous character. The highly metaluminous ( $\text{Al}/\text{NK} > 1.4$ ) character followed by metaluminous ( $\text{Al}/\text{NK} < 1.4$ ) and peraluminous nature of the Bahrah complex indicates a mixture of island arc and continental arc tectonic environments (Maniar and Piccoli 1989).

Figure 6 shows the CaO- $\text{Na}_2\text{O}$ - $\text{K}_2\text{O}$  diagram. The data points plot mainly in the tonalite and granodiorite fields (Condie and Hunter 1976). The sodic nature of the rocks of the Bahrah complex, with a dominating range (13-15%) of  $\text{Al}_2\text{O}_3$  contents, might indicate an oceanic environment (Baker 1979, Arth 1979, Jackson 1986). Also, the total alkali ( $\text{K}_2\text{O} + \text{Na}_2\text{O}$ ) versus  $\text{SiO}_2$  diagram (Fig. 7), shows that, in general, all the data points fall within the subalkaline field. However, points representing rocks of both ends of the fractionation series, *viz.*, quartz-diorites, fall mainly in

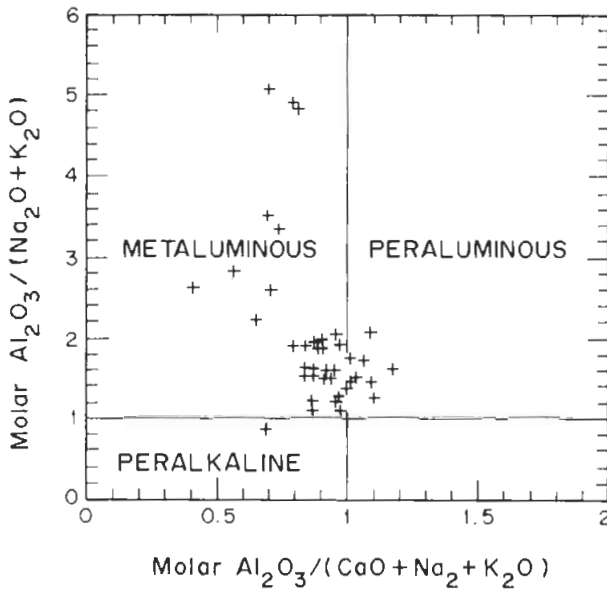


FIG. 5. Shand's index diagram shows the domination of metaluminous character.

the high alumina field, whereas granites fall mostly in the low alumina field. This is consistent with the metaluminous nature and oceanic type environment from the diagrams (Fig. 5 and 12).

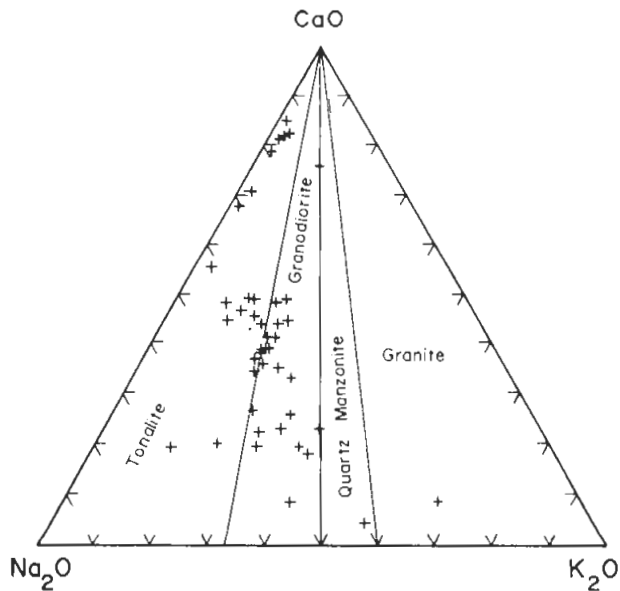


FIG. 6. CaO-Na<sub>2</sub>O-K<sub>2</sub>O diagram showing the calc-alkaline trend. The field boundaries are from Condic and Hunter (1976).

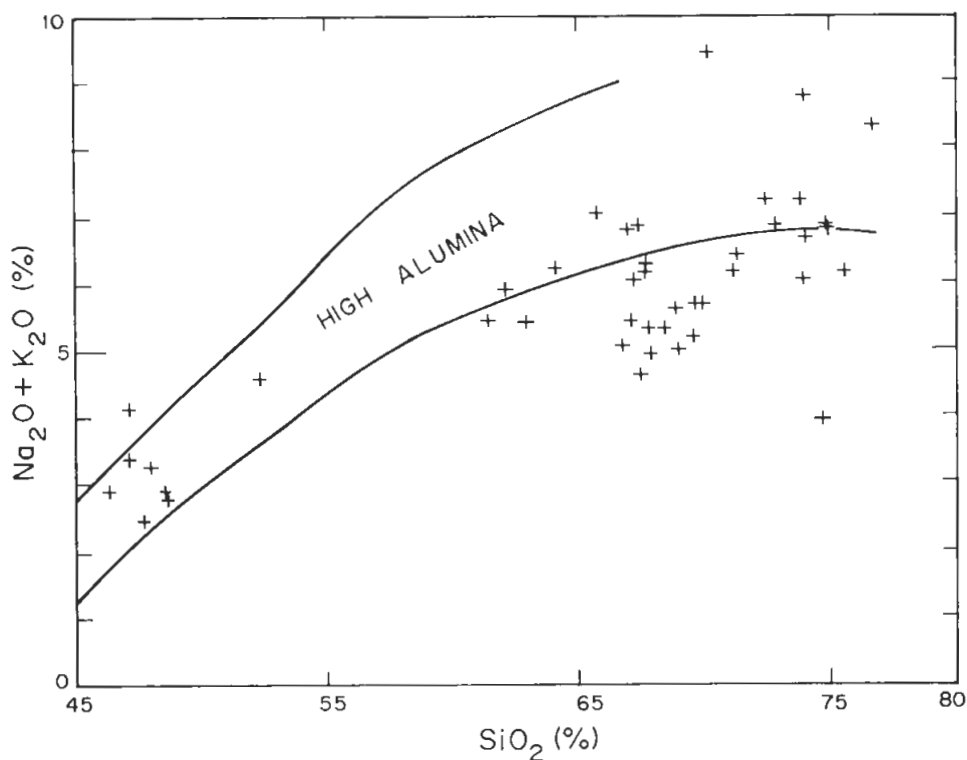


FIG. 7. Binary diagram showing distribution of alkali and silica, after Kuno (1968).

In the whole, the Bahrah granodiorite-granite complex has a variable  $\text{SiO}_2$  content, but high in  $\text{Na}_2\text{O}$ , and low in  $\text{CaO}$ ,  $\text{MgO}$ ,  $\text{K}_2\text{O}$  and  $\text{Fe}^{+3}/\text{Fe}^{+2}$  ratios. The  $\text{Al}_2\text{O}_3$  content is varying from oceanic environment ( $\text{Al}_2\text{O}_3 = 13\text{-}15\%$ ) to continental trondhjemite ( $\text{Al}_2\text{O}_3 > 15\%$ ) (Jackson 1986). The total Fe-content is moderate. These chemical features are quite similar to the group III younger granitoids which represent the early intrusions (700-600 Ma) within the emerging neo-crust of the Arabian Shield, characterized by calc-alkaline magmatic suites showing non iron-enrichment trends. These granitoids also are generally metaluminous.

#### Minor Elements

The variations in K, Rb, Sr and Ba, are shown in Fig. 8-10. In general, the complex rocks are high in Sr and Ba but low in Rb. This is typical of granitoids emplaced at deeper levels of the crust (Katazone). However, the K-Rb variation diagram (Fig. 9), indicates some enrichment of Rb than crustal average (74 ppm; Faure and Hurley 1963). This is supported by the large scatter of Rb observed above the liquid line of descent drawn on the Rb-Sr variation diagram (Fig. 8). The Ba-K (Fig. 10), relationship is consistent with the high pressure under which the pluton was emplaced (Grif-

fin and Murthy 1969). The K/Rb ratios range between 67 and 597 with an average and standard deviation of 248 and 102, respectively. Thirty-one samples out of 44 fall between 200 and 350. Most of the continental rocks have K/Rb ratios between 160 and 300, with an average of about 230 (Heier and Adams 1964). The large variation in the K/Rb values of the Bahrah complex may reflect the occurrences of strongly differentiated rocks ( $K/Rb < 160$ ; Heier and Taylor 1959, Kolbe and Taylor 1966) as well as rocks from oceanic environment ( $K/Rb > 300$ ; McDougall and Compston 1965).

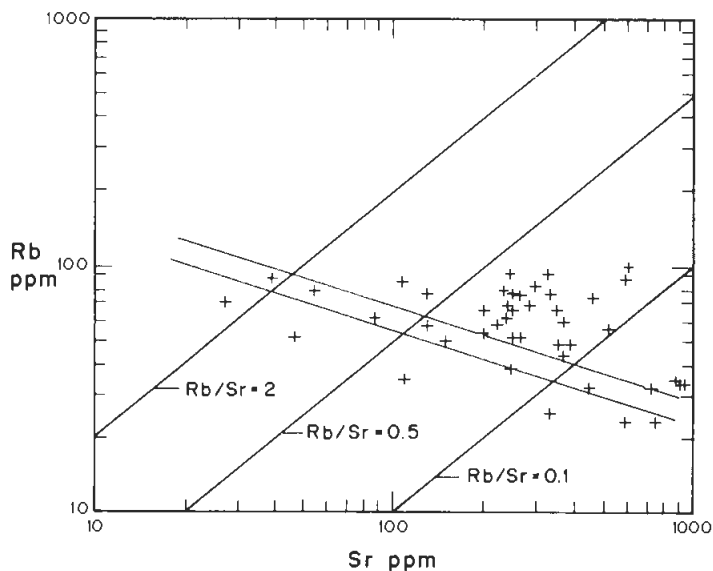


FIG. 8. Rb vs Sr log-log diagram. The band of the liquid line-of-descent is shown in the diagram.

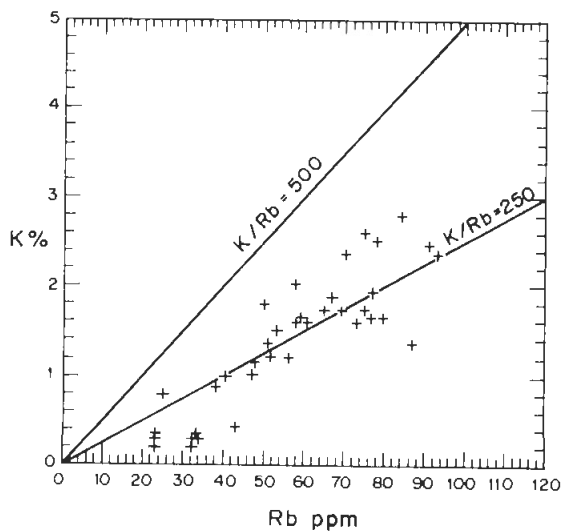


FIG. 9. K (wt%) vs Rb (ppm) variation diagram.

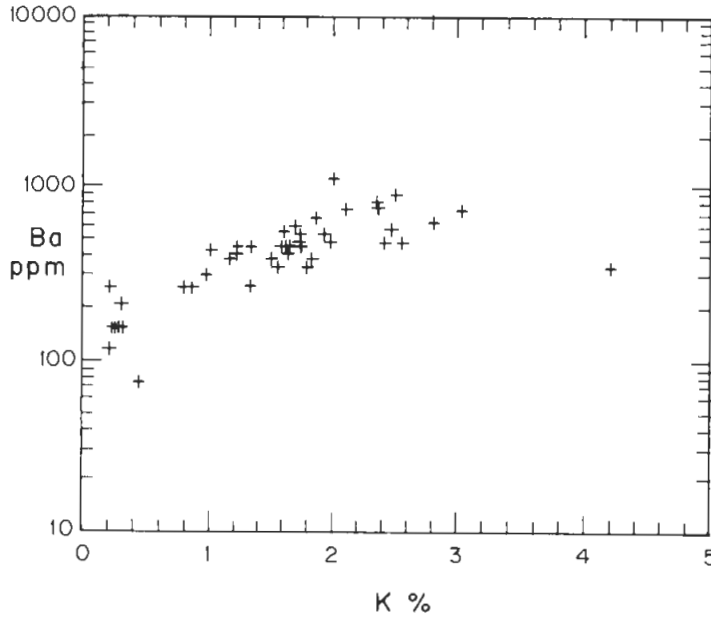


FIG. 10. Ba (ppm) vs K (wt%) variation diagram.

The variations of Rb, Y, and Nb versus  $\text{SiO}_2$  have been used as discriminate diagrams to indicate the tectonic regimes within which the magma developed (Pearce *et al.* 1984). Figure 11(a-c) show such variation diagrams for the Bahrah complex. The Rb- $\text{SiO}_2$  diagram (Fig. 11b) indicates that the Bahrah complex was developed either within volcanic island arc (VAG) or within plate (WPG) environments. The Y- $\text{SiO}_2$  diagram, (Fig. 11a) indicates that the complex evolved within volcanic island arc (VAG), collisional (COLG) or ocean ridge (ORG) environments. The Nb- $\text{SiO}_2$  diagram (Fig. 11c), indicates that the complex evolved within volcanic island arc (VAG), collisional (COLG), or ocean ridge (ORG) environments exactly as the Y- $\text{SiO}_2$  diagram. To carry the discrimination further to define the tectonic setting, the Nb-Y diagram (Fig. 12a) is used. The diagram indicates that the complex evolved in a volcanic island arc or syn-collisional type environments. Furthermore, the Rb-(Y + Nb) diagram (Fig. 12b) specifies that the Bahrah granodiorite complex developed within a volcanic island arc environment. This last designation is consistent with the interpretation of Camp (1984), Stoeser and Camp (1985) and Stoeser (1986) of the western regions of the Arabian Shield (central Hijaz region). These authors suggested crustal accretion by development of ensimatic island arcs followed by suturing and collisional events. The process of collision and the arc maturity thickened the crust which led to the development of granitoid plutonism of bimodal compositions. The early plutons are of calc-alkaline affinity which later changed into alkaline to peralkaline magmatism.

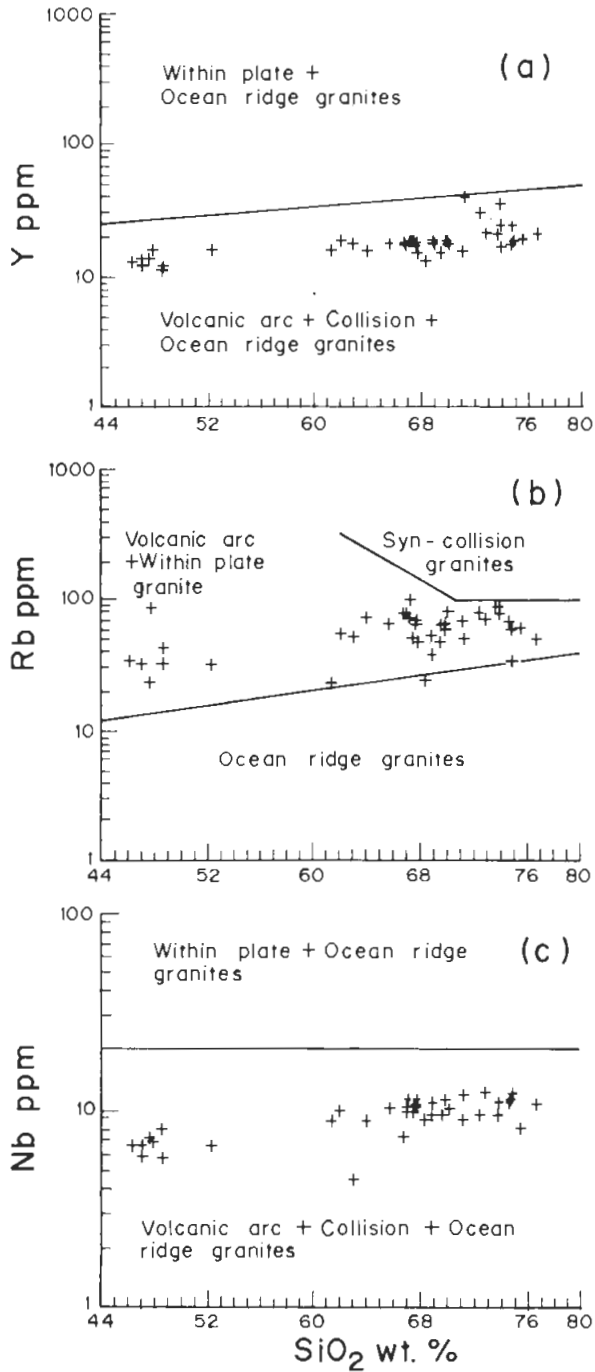


FIG. 11.  $\text{SiO}_2$ -trace elements tectonic discrimination diagrams (Pearce *et al.* 1984).

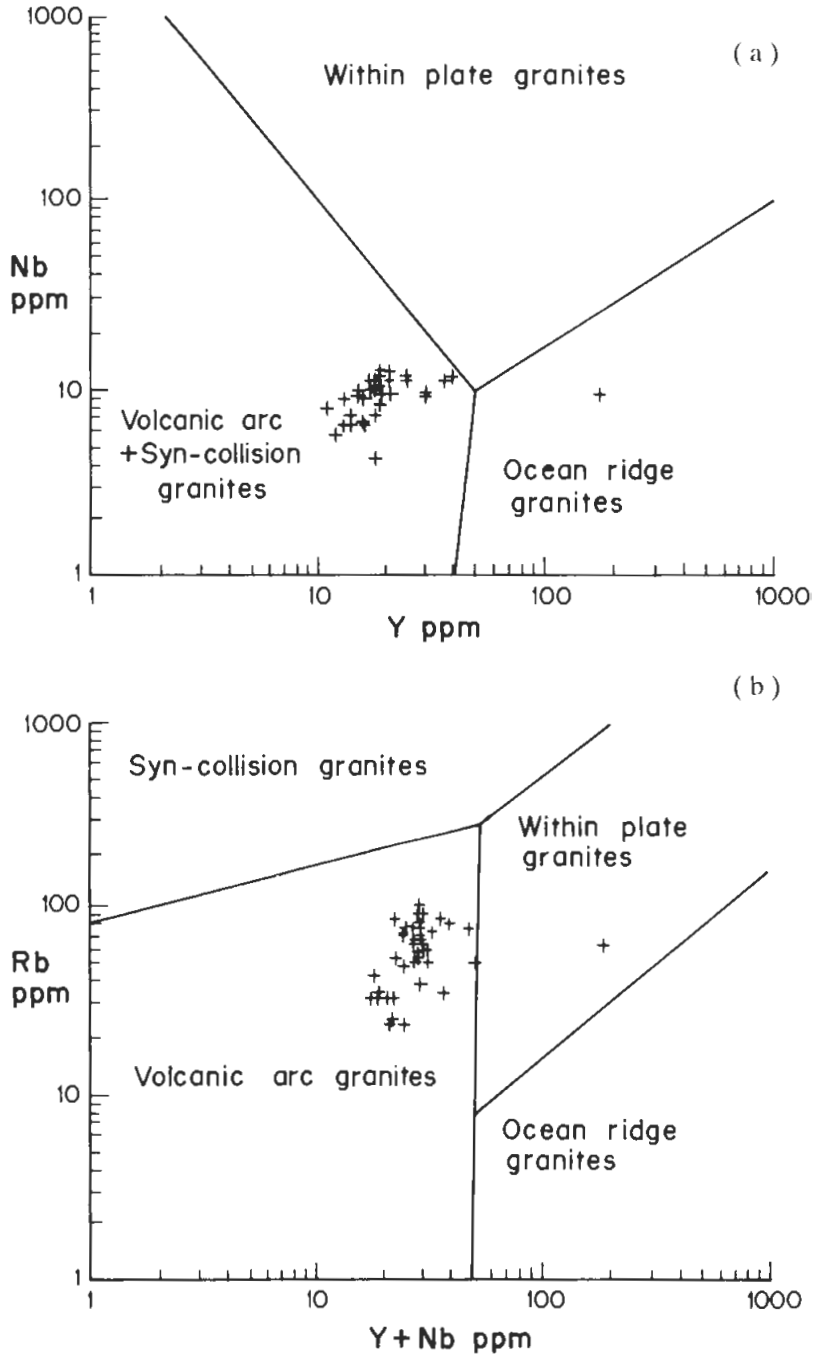


FIG. 12. Trace elements tectonic discrimination diagrams (Pearce *et al.* 1984).



### Rubidium-Strontium Geochronology

The samples of the granitic facies, especially along the N-S traverse, have been processed. The concentrations of Rb and Sr in the powdered samples were determined using XRF-spectrometric techniques. The Sr-isotopic compositions were measured using a VG-Isotopes 54E mass spectrometer. Regression of isochron data was done according to the techniques of York (1969). The decay constant for  $^{87}\text{Rb}$  ( $\beta = 1.42 \times 10^{-11} \text{Y}^{-1}$ ) was used to calculate the age of the pluton (Steiger and Jager 1977). The analytical data are shown in Table 2.

TABLE 2. Rb/Sr data of Bahrah granodiorite-granite complex.

Sample No.	Rb (ppm)	Sr (ppm)	$^{87}\text{Rb}/^{86}\text{Sr} \pm 2\sigma$	$^{87}\text{Sr}/^{86}\text{Sr} \pm 2\sigma$
MK-1	50.8	252.4	$0.5824 \pm .0058$	$0.707285 \pm .052$
MK-2	68.9	241.3	$0.8721 \pm .0083$	$0.710054 \pm .042$
MK-3	77.5	265.5	$0.8451 \pm .0085$	$0.710196 \pm .545$
MK-5	65.5	253.2	$0.7487 \pm .0075$	$0.709652 \pm .062$
MK-6	59.1	373.0	$0.4580 \pm .0046$	$0.706305 \pm .040$
MK-7	57.6	129.8	$1.2857 \pm .0129$	$0.713499 \pm .084$
MK-9	78.8	236.7	$0.9630 \pm .0096$	$0.711273 \pm .042$
MK-10	66.0	201.6	$0.9484 \pm .0095$	$0.710962 \pm .044$
MK-11	56.0	517.7	$0.3136 \pm .0031$	$0.704904 \pm .178$
MK-14	68.9	284.8	$0.7005 \pm .0070$	$0.723565 \pm .128$
MK-15	84.2	107.6	$2.2673 \pm .0227$	$0.708699 \pm .034$

The eleven points whole rock Rb/Sr isochron produced an age of  $664 \pm 12 \text{ Ma}$  for the Bahrah complex (Fig. 13), and an initial  $^{87}\text{Sr}/^{86}\text{Sr}$  ratio of  $0.70204 \pm 14$ . The MSWD value for the isochron is 0.09.

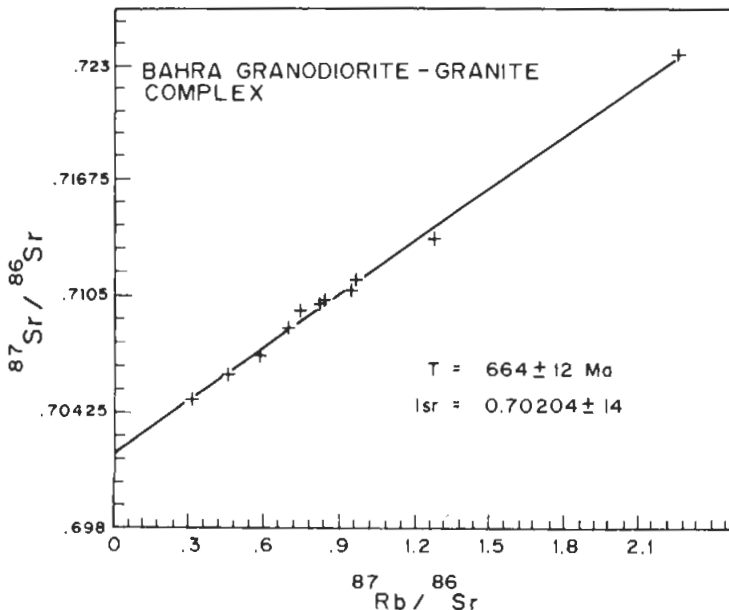


FIG. 13. Rb/Sr isochron plot for Bahrah granodiorite-granite complex.

This age classifies the Bahrah granodiorite-granite complex with the syntectonic plutonism of Hadiyah tectonic cycle defined by Kemp *et al.* (1980) in the western region of the Arabian Shield north of latitude 24°N. Similar ages have been also reported from the eastern region of the Shield by Abdel-Monem *et al.* (1989) for granodiorite-granitic pluton of the same geologic settings as well as petrochemical characteristics. Furthermore, ages in the range of 750-650 Ma, are reported from the same areas geologically mapped by Skiba (1980) for some granitoid intrusions. It is now suggested that in the geologic evolution of the Arabian Shield, the time span between 750-650 Ma, is characterized by the emplacement of deep seated (Katazonal) plutons ranging in composition from gabbroic-dioritic-quartz/dioritic-granodioritic to granitic, within the slightly (green-schist facies) volcano-sedimentary sequences. These plutons are sometimes exposed in the cores of gneiss domes. However, most of the time they are exposed as low relief negative geomorphologic features surrounded by high ridges of the metamorphosed volcano-sedimentary country rocks. Claesson *et al.* (1984) reported that the maximum age of the suturing or collisional event took place in the Arabian Shield between 780-740 Ma, by directly dating ophiolitic materials from Jabal Al-Wask and Jabl Ess ophiolite. This means that the series of plutonic rocks, that was emplaced between 750-650 Ma as outlined above, represent syn- to late-tectonic intrusions following the suturing episode.

The low initial  $^{87}\text{Sr}/^{86}\text{Sr}$  ratios, usually reported for this type of plutonic intrusives (0.702-0.703), indicate that they are either fresh additions from the upper mantle or by partial melting of deep crustal material with low Rb/Sr ratios and short history in the crust (Moorbath and Taylor 1981). The calc-alkaline nature and chemical characteristics of this suite of rock indicate their development near continental marginal arc such as the Andes (Pitcher 1982). However, the absence of any continental margin (Stoeser 1986) in the western arc terranes suggest their derivation from a thickened and matured ensimatic crust.

### **Acknowledgment**

This research was done with the financial support of the Saudi Arabian National Center for Science and Technology (SANCST), now known as King Abdulaziz City for Science and Technology (KACST), under Research Contract No. (AR-2-060). We wish to thank Mr. Syed Ali and Mr. M.S. Tashkendi for their assistance with the laboratory work. We also thank Dr. A.H. Hashad of the Faculty of Earth Sciences, King Abdulaziz University for reviewing the manuscript.

### **References**

- Abdel-Monem, A.A., Al-Shanti, A.M.S. and Radain, A.A. (1989) Rb/Sr geochronology of some gneisses and felsic intrusions from Afif-Halabab-Ad-Dawādimī-Ar-Rayn areas, Saudi Arabia, *J. King Abdulaziz University: Earth Sci.* **2** (in press).
- Aldrich, L.T. (1978) *Geochronologic Data for the Arabian Shield, Section I. Radiometric Age Determinations of Some Rocks from the Arabian Shield*, U.S. Geological Survey Saudi Arabian Project Report 240.

- Arth, J.G.** (1979) Some trace elements in trondhjemites, their implications to magma genesis and paleotectonic setting, *In: Barker, F. (ed.) Trondhjemites, Dacites, and Related Rocks*, Amsterdam. Elsevier, 123-132.
- Barker, F.** (1979) Trondhjemite-definition, environment and hypothesis of origin. *In: Barker, F. (ed.) Trondhjemites, Dacites and Related Rocks*, Elsevier, Amsterdam, 1-12.
- Brown, G.F., Jackson, R.O., Bogue, R.G. and Maclean, W.H.** (1963) *Geological Map of the Southern Hijaz Quadrangle, Kingdom of Saudi Arabia*, U.S. Geol. Surv. Misc. Geol. Investigations, Map I-210 A, Scale 1:500,000.
- Camp, V.E.** (1984) Island arcs and their role in the evolution of the western Arabian Shield, *Bull. Geol. Soc. Am.* **95**: 913-921.
- Claesson, S., Pallister, J.S. and Tatsumoto, M.** (1984) Samarium-Neodymium data on two late Proterozoic ophiolites of Saudi Arabia and implications for crustal and mantle evolution, *Contrib. Mineral. Petrol.* **85**: 244-252.
- Condie, K.C. and Hunter, D.R.** (1976) Trace element geochemistry of Archean granitic rocks from the Barberton region, South Africa, *Earth Planet. Sci. Lett.* **29**: 389-400.
- Faure, G. and Hurley, P.M.** (1963) The isotopic composition of strontium in oceanic and continental basalts; Application to the origin of igneous rocks. *Petrol. J.* **4**: 31-50.
- Fleck, R.J.** (1981) *Age of Diorite-Granodiorite Gneisses of the Jeddah-Makkah Region, Kingdom of Saudi Arabia*, Saudi Arabian Deputy Ministry for Mineral Resources Open-File Report USGS-OF-01-1, 18 p.
- Fleck, R.J., Greenwood, W.R., Hadley, D.G., Anderson, R.E. and Schmidt, D.L.** (1980) *Rubidium-Strontium Geochronology and Plate-tectonic Evolution of the Southern Part of the Arabian Shield*, U.S. Geological Survey Professional Paper 1131, 39 p.
- Griffin, W.L. and Murthy, V.R.** (1969) Distribution of K, Rb, Sr, and Ba in some minerals relevant to basalt genesis, *Geochim. Cosmochim. Acta* **33**: 1389-1414.
- Heier, K.S. and Adams, J.A.S.** (1964) The geochemistry of the alkali metals, *Phys. Chem. Earth* **5**: 253-381.
- Heier, K.S. and Taylor, S.R.** (1959) Distribution of Li, K, Rb, Cs, Pb, and Tl in southern Norwegian pre-Cambrian alkali feldspar, *Geochim. Cosmochim. Acta* **15**: 284-304.
- Irvine, T.N. and Baragar, W.R.A.** (1971) A guide to the chemical classification of the common volcanic rocks. *Canad. J. Earth Sci.* **8**: 523-548.
- Jackson, N.J.** (1986) Petrogenesis and evolution of Arabian plutonic rocks. *J. Afr. Earth Sci.* **4**: 47-59.
- Jackson, N.J., Douch, C.J., Odell, J., Bedawi, H., Al-Hazmi, H., Pegram, E. and Walsh, J.N.** (1984a) Late Precambrian granitoid plutonism and associated mineralization in the central Hijaz. *Fac. Earth Sci., King Abdulaziz Univ.*, *Bull.* **6**: 512-537.
- Jackson, N.J., Walsh, J.N. and Pegram, E.** (1984b) Geology, geochemistry and petrogenesis of Late Precambrian granitoids in the central Hijaz region of the Arabian Shield. *Contrib. Mineral. Petrol.* **87**: 205-219.
- Keimp, J., Pellaton, C. and Calvez, J.Y.** (1980) *Geochronological Investigations and Geological History in the Precambrian of North-Western Saudi Arabia*, Saudi Arabian Deputy Ministry for Mineral Resources Open-File Report BRGM-OF-01-1.
- Kolbe, P. and Taylor, S.R.** (1966) Major and trace elements relationships in granodiorites and granites from Australia and South Africa, *Contr. Mineral. and Petrol.* **12**: 202-222.
- Kuno, H.** (1968) Origin of andesites and its bearing on the island arc structure, *Bull. Volcanol.* **32**: 141-176.
- Maniar, P.D. and Piccoli, P.M.** (1989) Tectonic discrimination of granitoids, *Geol. Soc. Am. Bull.* **101**: 635-643.
- McDougall, I. and Compston, W.** (1965) Strontium isotope composition and potassium-rubidium ratios in some rocks from Reunion and Rodriguez, Indian Ocean. *Nature* **207**: 252-253.
- Moorbath, S. and Taylor, P.N.** (1981) Isotopic evidence for continental growth in the Precambrian. *In: Kroner, A. (ed.) Precambrian Plate Tectonics*, Elsevier Scientific Publishing Company, Amsterdam, pp. 491-525.

- Pearce, J.A., Harris, N.B.W. and Tindle, A.G.** (1984) Trace element discrimination diagrams for the tectonic interpretation of granitic rocks, *J. Petrol.* **25**: 956-983.
- Pitcher, W.S.** (1982) Granite type and tectonic environment. In: **Hsu, K.J. (ed.)** *Mountain Building Processes*, Academic Press, London, pp. 19-40.
- Shand, S.J.** (1951) *Eruptive Rocks*, John Wiley, New York.
- Skiba, W.J.** (1980) The form and evolution of late Precambrian plutonic rocks in the Jeddah-Rabigh-Wadi Al-Qahah area, Saudi Arabia. In: **Al-Shanti, A.M. (Convenor)** *Evolution and Mineralization of the Arabian Shield*, *Bull. Inst. Appl. Geol., King Abdulaziz Univ., Jeddah*, No. 3, Pergamon Press, Oxford, 105-120.
- Steiger, R.H. and Jager, E.** (1977) Subcommittee on geochronology: convention on the use of decay constants in geo- and cosmo-chronology, *Earth Planet. Sci. Lett.* **36**: 359-362.
- Stoeser, D.B.** (1986) Distribution and tectonic setting of plutonic rocks of the Arabian Shield, *J. Afr. Earth Sci.* **4**: 21-46.
- Stoeser, D.B. and Camp, V.E.** (1985) Pan-African microplate accretion of the Arabian Shield, *Bull. Geol. Soc. Am.* **6**: 817-826.
- Tuttle, O.F. and Bowen, N.L.** (1958) Origin of granites in the light of experimental studies in the system  $\text{NaAlSi}_3\text{O}_8\text{-KAlSi}_3\text{O}_8\text{-SiO}_2$ , *Geol. Soc. Am. Mem.* **74**: 153 p.
- York, D.** (1969) Least-squares fitting of a straight line with correlated errors, *Earth Planet. Sci. Lett.* **5**: 320-324.

## عمر وكيمياء الصخر لمعقد بحرة من الجرانوديوريت - جرانيت بمنطقة جدة - مكة - المملكة العربية السعودية

عبد العزيز رادين\* ، أحمد السنطي\* و عبد الله عبد المنعم\*  
\* كلية علوم الأرض ، جامعة الملك عبد العزيز - جدة ، المملكة العربية السعودية  
\*\* هيئة المواد النووية - جمهورية مصر العربية

مستخلص . يُشكل معقد بحرة من الجرانوديوريت - جرانيت محقوناً بيضياً باتجاه شمال شرق - جنوب غرب على هيئة تضاريس منخفضة نسبياً عند تقاطع وادي فاطمة إلى الغرب و وادي الشميسي إلى الشرق . وتُحده من الغرب مجموعة جدة من البركانيات المتحولة ومجموعة باحة من التست الرسوبي الأصل . أما من الشرق ، فيلامس المعقد مجموعة جدة من البركانيات المتحولة وما يتداخل فيها من ديوريت كوارتزي . ويقطع المعقد مجموعة من الجدد القاعدية دقيقة الحبيبات باتجاه شرق - غرب .

تتراوح سحنات المعقد بين الجابرو والجرانيت ، أما النوع الرئيس فهو جرانيت بيوتيتي ، بالإضافة إلى الهورنبلند أحياناً ، متوسط إلى خشن الحبيبات . أما سحنات الديوريت الكوارتزي والجرانوديوريت قرب حواف المعقد فهي متورقة وتحتوي مكتنفات كثيرة داكنة موضحة أن آلية التوضع كانت بالالتهام .

تميل هذه المحقونات إلى الطبيعة الكلس قلوية الغنية بالألومنيوم ، في حين تبدو عناصر ليل (العناصر الأيونية الكبيرة للغللاف الصخري) مستنزفة بدرجة كبيرة مما يوحي بنشأة للصهار مرتبطة بعملية انضواء .

قُدِّر عمر المعقد بطريقة الرابديوم - استرنشيوم بـ  $665 \pm 12$  مليون سنة ويُفسر بأنه عمر التوضع خلال الفترة الزمنية التي أعقبت ترسب مجموعة فاطمة والتي يقدر عمرها بـ 690 - 680 مليون سنة . ويكافئ هذا العمر زمنياً الدورة التداخلية والحركات التكوينية التي أعقبت ترسب مجموعات حلبان وحليفة ذات الانتشار الواسع في الدرع العربي .